Short Papers

Predistortion Techniques for Multicoupled Resonator Filters

A. E. WILLIAMS, W G. BUSH, AND R. R. BONETTI

Abstract —**This paper presents predistorted, lossy design techniques as applied to general, multicoupled, resonator networks. The analytical procedure predistorts the poles of the transfer function to recover the lossless passband flatness at the expense of insertion loss. Experimental results on 4- and 6-pole elliptic-function filters confirm the validity of the theory. These techniques should lead to significant system efficiencies in applications such as satellite transponder input multiplexers.**

I. INTRODUCTION

A standard multicoupled-cavity filter employs synchronously tuned resonators coupled via apertures to produce the desired transfer function. Typically, the synthesis procedure assumes that the resonator losses are sufficiently minimal to realize a transfer response that is only marginally different from the lossless theoretical functions. This assumption is invalid, however, for designs with low cavity Q's or bandwidths that are very small compared to the center frequency. Under these conditions, significant band-edge rounding of the response occurs. In some applications, such as when a filter precedes a nonlinearity in a satellite transponder, this rounding can lead to severe degradation in communications system performance.

In 1939, Darlington [1] showed that the lossless insertion loss response of a network could be essentially recovered by realizing a transfer function whose poles were shifted to compensate for the network loss. Previous works [2],[3] applied this technique to the realization of all pole functions in coupled microwave resonators. This paper extends this theory to optimum filter transfer functions, which have poles and finite zeros. Experimental results on a narrow-band 12-GHz, 4-pole filter and a C-band, 6-pole dielectric-loaded filter are in good agreement with the theory.

II. THEORY OF POLE PREDISTORTION

The general low-pass insertion loss function $t(s)$ that can be synthesized by coupled cavities is given by

$$|t(s)|^2 = \left[1+\epsilon^2(-1)^n s^{2n}\frac{\prod_{k=1}^{m}\left(s^2+z_k^2\right)^2}{\prod_{k=1}^{l}\left(s^2+p_k^2\right)^2}\right]^{-1} \tag{1}$$

with the constraint $n+2m+1 \geqslant 2l$. This function can be determined from $|t(s)|^2 = t(s)\cdot t(-s)$, giving

$$t(s) = \frac{1}{\epsilon}\frac{\prod_{k=1}^{l}\left(s^2+p_k^2\right)}{\prod(s-v)} \tag{2}$$

where v represents the poles of the transfer function and $\prod(s-v)$ is a Hurwitz polynomial.

Since $|\rho(s)|^2 = 1-|t(s)|^2$ and $|\rho(s)|^2 = \rho(s)\cdot\rho(-s)$

$$\rho(s) = (-1)n_s n\frac{\prod_{k=1}^{m}\left(s^2+z_k^2\right)}{\prod(s-v)}. \tag{3}$$

The actual response of a real filter will differ from $t(s)$ and $\rho(s)$ because losses are present in the structure. Assuming uniform dissipation, the circuit model is modified to include a loss resistance r in each resonator. This gives the model shown in Fig. 1. The resulting low-pass functions are then obtained by replacing s with $s+r$, which causes the frequency axis to shift to the right in the s-plane, where r is given by

$$r = \frac{1}{Q_u\cdot F_{BW}}. \tag{4}$$

Q_u is the unloaded resonator Q, and F_{BW} represents the fractional bandwidth. The transfer and reflection functions that result in the presence of loss [$t'(s)$ and $\rho'(s)$] are, therefore, given by

$$t'(s) = t(s+r)$$
$$\rho'(s) = \rho(s+r)$$

and the dissipated power by

$$|\Delta'(s)|^2 = 1-|t'(s)|^2-|\rho'(s)|^2.$$

The most straightforward way to counter this loss is to displace all the poles and zeros of $t(s)$ by r in the z-plane. However, since coupled-cavity resonator networks require zeros on the imaginary axis, only the poles can be predistorted. Fortunately, this has only a small effect on the in-band behavior of the filter, since the zeros mainly affect the out-of-band behavior. It should be noted that the poles cannot be shifted out of the left half of the s-plane. Thus, in cases where r is quite large, a good design can often be obtained by partial predistortion (preshifting the poles by some fraction of r).

Full predistortion results in a transfer function $t_p(s)$ given by

$$t_p(s) = K\cdot\frac{1}{\epsilon}\frac{\prod\left(s^2+p^2\right)}{\prod[s-(v+r)]} \tag{5}$$

where K is introduced to ensure that $t_p(s)$ has a maximum magnitude of unity. Fig. 2 illustrates the pole predistortion of a 6-pole, elliptic-function filter, and the effect on the transmission and return loss is shown in Figs. 3 and 4. The group delay of the lossless filter is essentially recovered by the predistorted process.

Two properties of this procedure are important to the filter design. As shown in Fig. 4, pole predistortion increases the amount of power reflected and the insertion loss of the network. These effects can be understood in terms of the design process. In the predistorted, lossless case, the band-edges of the transmission response are considerably higher than the center. This is necessary to give the resulting filter (with loss present) a flat in-band response. The introduction of loss attenuates the band-edges more than the center of the band, so the response flattens out.

Manuscript received May 7, 1984; revised December 10, 1984. This paper is based on work performed at COMSAT Laboratories, Clarksburg, MD 20871, under the sponsorship of the Communications Satellite Corporation.

A. E Williams and R. R Bonetti are with COMSAT Laboratories, Clarksburg, MD 20871

W. G. Bush was with COMSAT Laboratories, Clarksburg, MD. He is now with Aerospace Corporation, El Segundo, CA

0018-9480/85/0500-0402$01.00 ©1985 IEEE

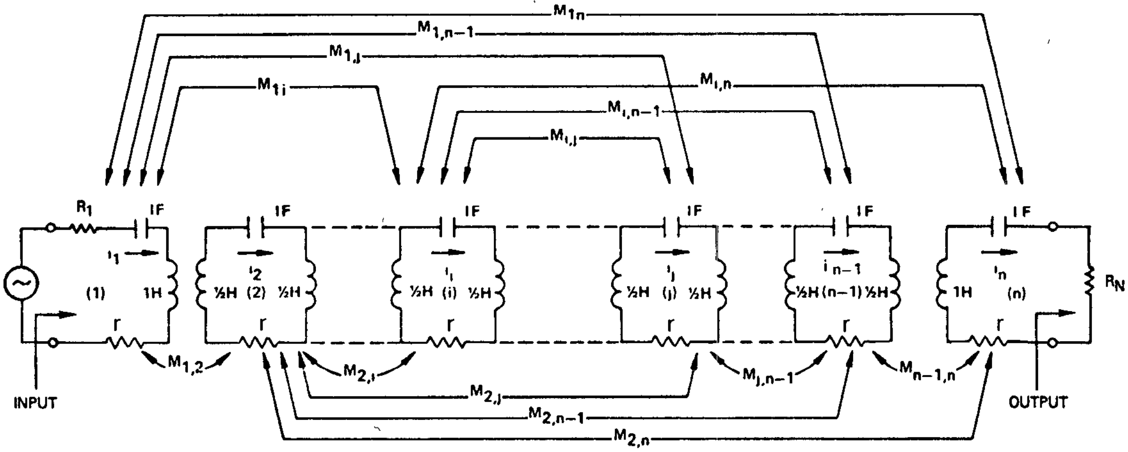

Fig 1. Equivalent circuit of n-coupled cavities with uniform dissipation.

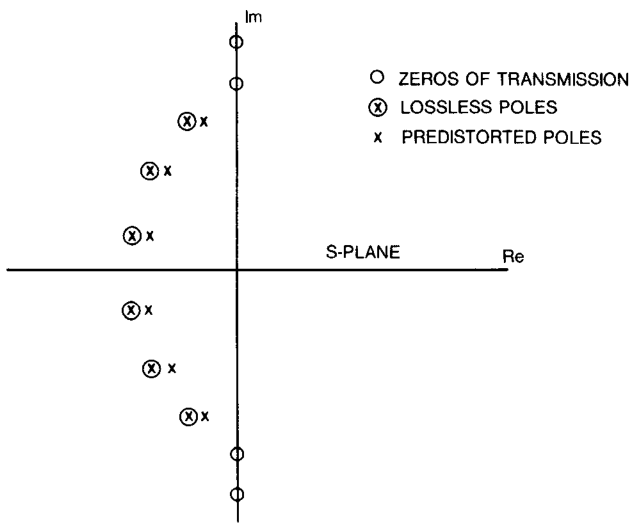

Fig. 2. Typical location of poles and zeros for a 6-pole elliptic-function bandpass filter.

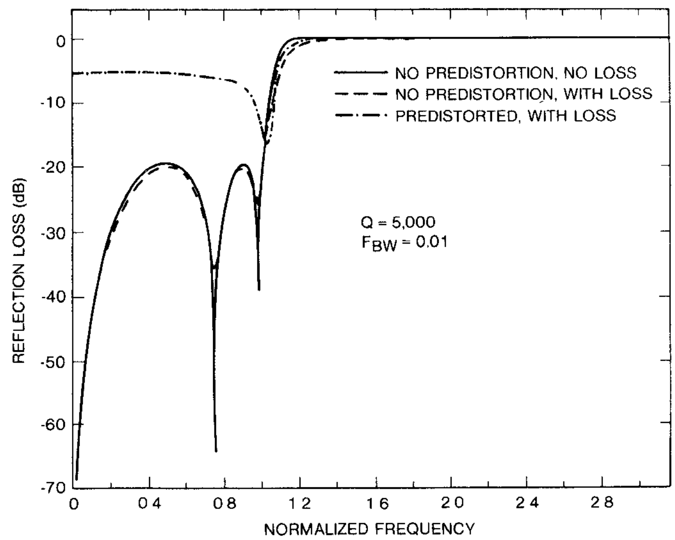

Fig. 4. Theoretical return loss responses of a 6-pole elliptic-function filter

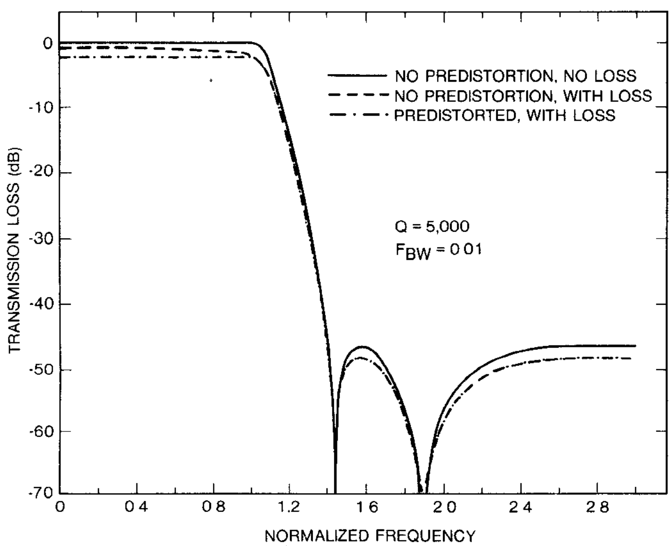

Fig. 3. Theoretical transmission responses of a 6-pole elliptic-function filter.

Pole predistortion is, therefore, limited to those applications where minimum insertion and maximum return loss are not required.

Several other effects can be examined in terms of the transfer function pole locations. For elliptic-function filters, the behavior of the pole closest to the frequency axis dominates the band-edge response. It is largely the movement of this pole in the lossy, nonpredistorted design that leads to rounding of the band-edge. If this pole pair occurs at $s = -a \pm jb$, a good approximation of the center frequency insertion loss L_{FC} that will result with a predistorted design is

$$L_{FC} \cong 20\log\left(\frac{a-r}{a}\right), \qquad a > r. \tag{6}$$

Thus, more selective filters will demonstrate greater insertion losses by using predistortion, since the poles are closer to the real axis. The real part of this pole also limits the amount of predistortion that can be applied. The use of (6) will give a good initial indication of whether full or partial predistortion of the network is the most desirable.

III. Synthesis

The synthesis of the predistorted transfer function (5) is nearly identical to that described by Atia, Williams, and Newcomb [4]. Using Darlington's notation [1], the lossless low-pass transfer function is expressed as

$$t(s) = \frac{P(s)}{A(s) + sB(s)} \tag{7}$$

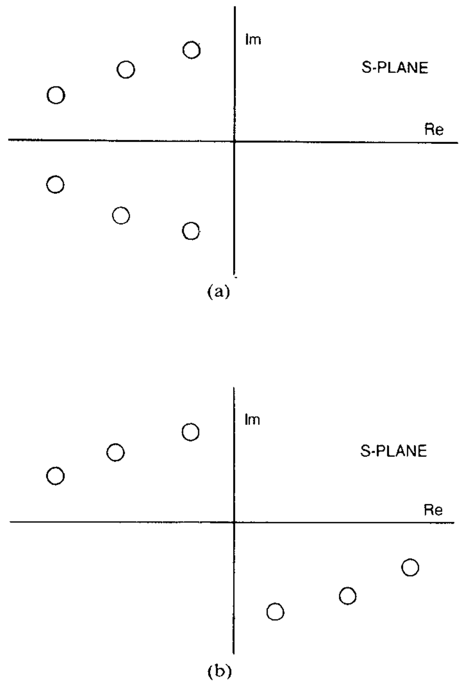

Fig. 5. Examples of reflection zero choices for synchronous and asynchronous realizations. (a) Synchronous. (b) Asynchronous.

and the reflection as

$$\rho(s)=\frac{A'(s)+sB'(s)}{A(s)+sB(s)} \tag{8}$$

where $A(s)$, $A'(s)$, $B(s)$, $B'(s)$, and $P(s)$ are all even polynomials. The general short-circuit admittances are

$$Y_{11}=\frac{1}{R_1}\frac{-j\,\mathrm{Im}[A'(s)]+s[B(s)-B'(s)]}{A(s)+\mathrm{Re}[A'(s)]}$$

$$Y_{n1}=\frac{-1}{\sqrt{R_n R_l}}\frac{P(s)}{A(s)+\mathrm{Re}[A'(s)]}$$

$$Y_{nn}=\frac{1}{R_n}\frac{j\,\mathrm{Im}[A'(s)]+s[B(s)+B'(s)]}{A(s)+\mathrm{Re}[A'(s)]}. \tag{9}$$

The coupling matrix is constructed from the residues of Y_{11} and Y_{nn} evaluated at the roots of the polynomial $A(s) + \mathrm{Re}[A'(s)]$. The type of solution that results depends on the choice of reflection zeros derived from the relation $|\rho(s)^2 = \rho(s) \cdot \rho(s)$. For the conventional, nonpredistorted design, all reflection zeros lie on the imaginary axis, so only one choice exists. This results in

$$\mathrm{Im}[A'(s)]=B'(s)=0. \tag{10}$$

Thus, the residues of Y_{11} and Y_{nn} are equivalent, and a symmetrical filter results.

In the predistorted design, a choice can be made in selecting the reflection zeros. If total left- or right-half plane zeros are chosen, then

$$\mathrm{Im}[A'(s)]=0. \tag{11}$$

The residues of Y_{11} and Y_{nn} will be real, but they will differ. Thus, an asymmetric, synchronously tuned filter will be realized. If a combination of left- and right-half plane zeros is chosen, the result is

$$B'(s)=0. \tag{12}$$

The real parts of the residues will be equivalent, so the couplings and resistances will be symmetrical. However, the introduction of a nonzero imaginary part in the admittances will cause the solution to be asynchronous. This means that the cavities will be tuned to frequencies that are slightly offset from the filter center frequency. The sum of these mistunings will be zero for a filter with a frequency response that is symmetrical about its center frequency.

Fig. 5 illustrates examples of possible reflection zero choices. Typically, a total left- or right-half plane set is chosen to simplify the tuning process. However, in cases where this choice dictates coupling or resistance values that may be difficult to realize, the asynchronous solution may be the most attractive.

IV. Sixth-Order Filter Design

As a design example, the predistortion of a 6-pole elliptic function filter is presented. Assuming an in-band ripple of 0.15 dB and a selectivity of 1.135, the poles of the transfer function are

$$-0.6333 \pm j0.4150$$
$$-0.2329 \pm j0.9107$$
$$-0.0464 \pm j1.0264.$$

For the application of a very narrow-band filter with a fractional bandwidth of 0.734 percent and a Q of 8000, the pole shift will be $r = 0.0170$. Full-pole predistortion can be used, and as an approximation, the insertion loss will be about

$$L_{FC} \cong 20\log\left[\frac{0.0464-0.0170}{0.0464}\right] = 3.96 \text{ dB}.$$

The new transfer function poles are

$$-0.6163 \pm j0.4150$$
$$-0.2159 \pm j0.9107$$
$$-0.0294 \pm j1.0264.$$

The zeros of the transfer function (before and after predistortion) are $\pm j1.1553$ and $\pm j1.4273$.

Choosing all left-half plane reflection zeros, the Darlington polynomials become

$$A(s) = s^6 + 3.10s^4 + 2.62s^2 + 0.51$$
$$B(s) = 1.72s^4 + 3.18s^2 + 1.41$$
$$P(s) = 0.13s^4 + 0.43s^2 + 0.34$$
$$A'(s) = s^6 + 2.69s^4 + 2.07s^2 + 0.37$$
$$B'(s) = 1.46s^4 + 2.55s^2 + 1.08.$$

Note that $\mathrm{Im}[A'(s)] = 0$ and $B'(s) \neq 0$. Thus, the resulting filter will be synchronously tuned, but its couplings and resistances will not be symmetrical.

Evaluating the residues of the short-circuit admittances at the roots of $\{A(s) + \mathrm{Re}[A'(s)]\}$ and rotating the resulting matrix to the desired form, the normalized couplings and resistances are found to be

$R_1 = 1.588$	$M_{45} = -0.852$
$R_6 = 0.130$	$M_{56} = 0.559$
$M_{12} = 1.037$	$M_{16} = -0.139$
$M_{23} = -0.672$	$M_{36} = -0.411.$
$M_{34} = -0.379$	

With these values, the implemented filter showed an insertion loss of 4.0 dB.

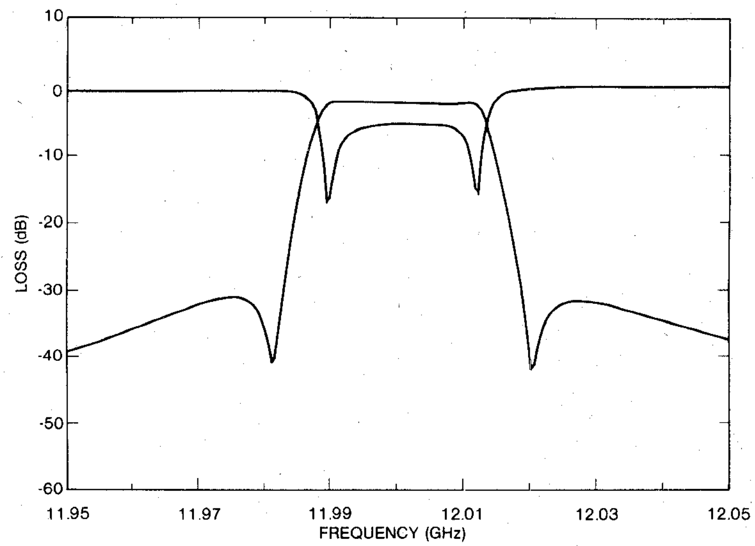

Fig. 6. Transmission and return loss response of a predistorted, 12-GHz 20-MHz bandwidth 4-pole elliptic-function filter.

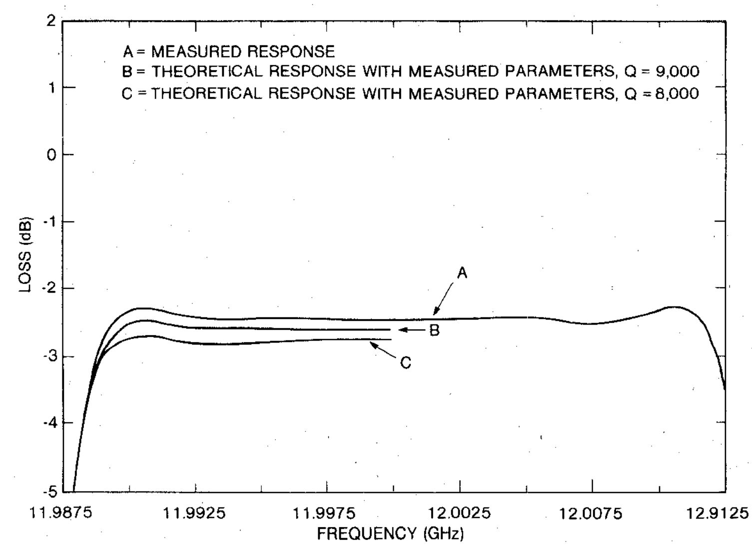

Fig. 7. In-band transmission responses of a predistorted, 12-GHz 20-MHz bandwidth 4-pole elliptic-function filter.

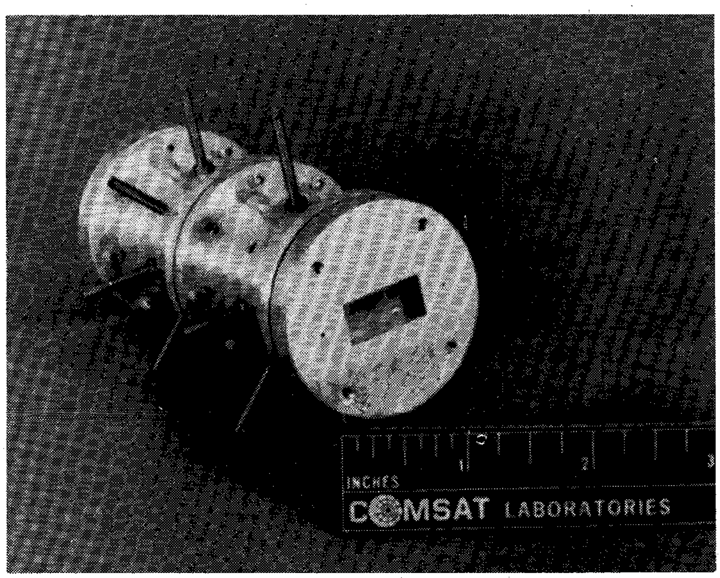

Fig. 8. A 12-GHz 4-pole predistorted elliptic-function filter.

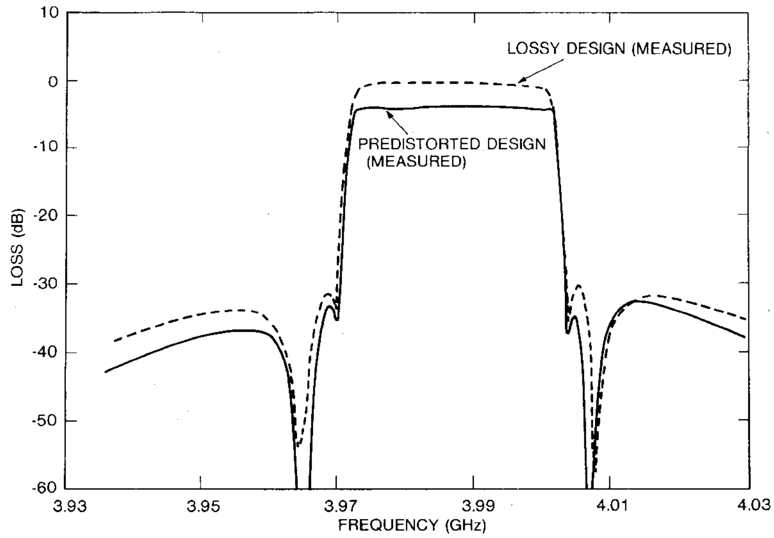

Fig. 9. Transmission response of lossy and predistorted 6-pole C-band elliptic-function filters.

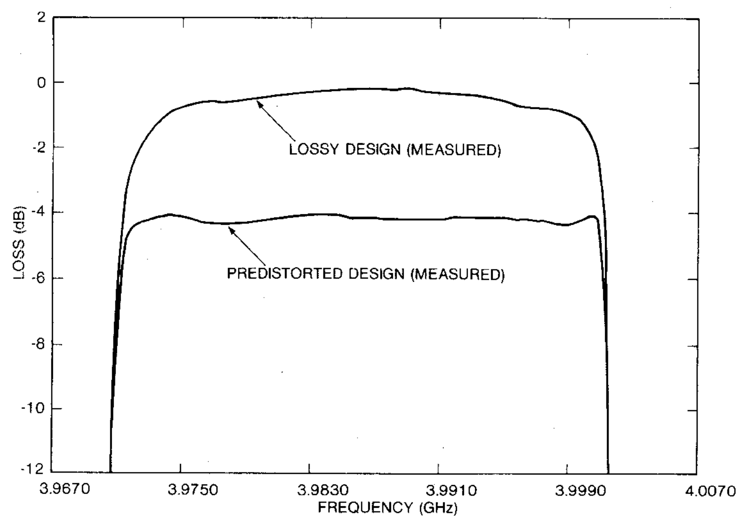

Fig. 10. In-band transmission responses of lossy and predistorted 6-pole C-band elliptic-function filters.

Since the Q may not be exactly known before the filter is constructed, several iterations may be necessary. However, assuming a fairly good initial estimate of the Q, the parameter values should change only slightly.

V. Experimental Filters

A 20-MHz bandwidth, 4-pole, elliptic-function, predistorted filter with a center frequency of 12 GHz was designed to operate in dual TE_{113}-moded aluminum cavities. For a Q of 8000, the pole predistorted design factor $r = 1/(Q_u F_{BW}) = 0.075$. The asymmetrical set of couplings was derived, and the physical cavity dimensions were determined by using standard lossless filter design techniques. The experimental insertion and return loss of the filter is shown in Fig. 6, and the in-band insertion loss is shown in Fig. 7. The measured response corresponds to a cavity Q in excess of 9000. Fig. 8 is a photograph of this filter.

To further illustrate the effects of predistortion, two 6-pole elliptic filters were designed with the dual $HE_{11}\delta$ dielectric-loaded cavity mode. The first filter was designed by using conventional lossy techniques [4], and the second filter design was derived from the numerical example given in the previous section. Both designs had a center frequency of 3.986 GHz, a bandwidth of 29 MHz, and an unloaded Q of 8000. The measured responses for both units are compared in Figs. 9 and 10. The effects of predistortion are clearly evident. Fig. 11 is a photograph comparing the size of a C-band, air-filled, dual-mode cavity filter and the C-band, dual-mode dielectric-loaded cavity filter.

It should be emphasized that, because of the poor return loss generated by the predistortion process, high-quality circulators (with return loss greater than 35 dB and VSWR less than 1.04) must be used with predistortion filters.

VI. Conclusions

Predistortion pole techniques, as applied to optimum filter transfer functions, are successfully realized in general microwave-coupled resonator structures. Symmetrical asynchronous and asymmetrical synchronous solutions are derived. Techniques such as these can lead to significant improvements in system efficiencies for applications such as satellite transponder input multiplexers, where insertion loss can be traded for in-band flatness.

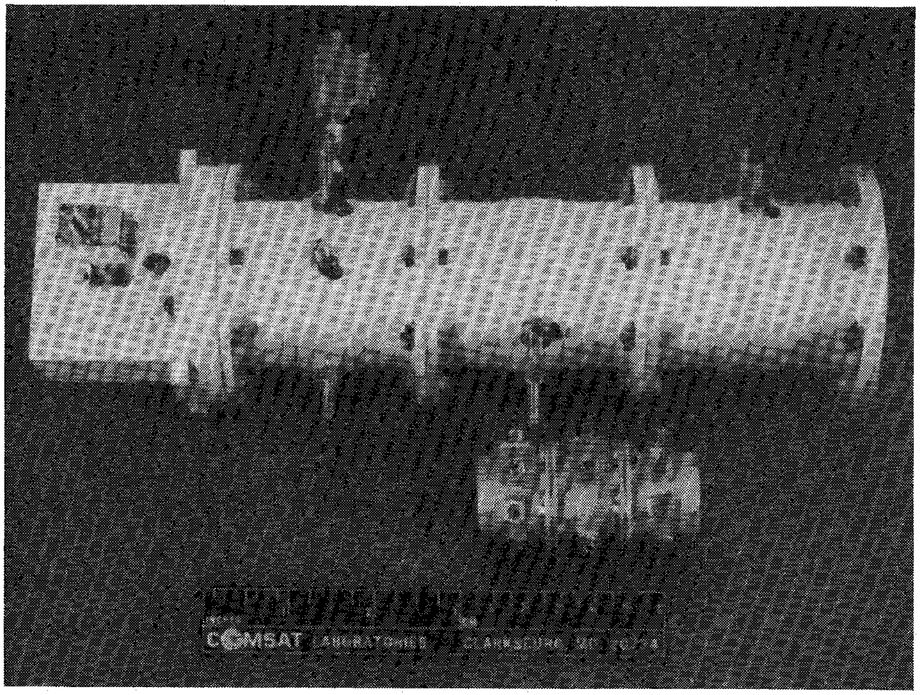

Fig. 11. Comparison of the C-band dual-mode dielectric-function filter and a C-band air-filled dual-mode filter.

REFERENCES

[1] S. Darlington, "Synthesis of reactance—Four poles which produce prescribed insertion loss characteristics," *J. Math. Phys.*, vol. 18, Sept. 1939.

[2] R. M. Livingston, "Predistorted waveguide filters," *G-MTT Int. Microwave Symp., Dig.*, 1969, pp. 291–297.

[3] M. H. Chen and C. E. Mahle, "Design of a lossy waveguide filter," *COMSAT Tech. Rev.*, vol. 5, no. 2, pp. 387–398, 1975.

[4] A. E. Atia, A. E. Williams, and R. W. Newcomb, "Narrowband multiplexer-coupled cavity synthesis," *IEEE Trans. Circuits Sys.*, vol. CAS-21, pp. 649–655, Sept. 1974.

Singularity Extraction from the Electric Green's Function for a Spherical Resonator

M. BRESSAN AND G. CONCIAURO

Abstract —**The electric dyadic Green's function for a spherical resonator is expressed as a sum of two dyadics given in closed form and a dyadic given in the form of a series. The first two dyadics diverge at the source point and they represent a low-frequency approximation for the Green's function, valid up to frequencies moderately lower than the resonant frequency of the dominant mode. The dyadic given in the form of a series is finite at the source and takes into account cavity resonances. It is given either as a one-index series, whose terms are transcendental functions of the frequency, or as a double series, whose terms are rational functions of the frequency. Both series have very good converging properties everywhere inside the cavity.**

I. INTRODUCTION

The electric field at any point inside a cavity resonator bounded by a perfectly conducting wall, filled with a linear, isotropic, homogeneous medium with constitutive parameters ϵ, μ, and excited by time-harmonic ($\exp j\omega t$) electric sources may be expressed as

$$\boldsymbol{E}(\boldsymbol{r}) = -j\omega\mu \lim_{\delta \to 0} \int_{V-V_\delta} \overline{\boldsymbol{G}}_e(\boldsymbol{r},\boldsymbol{r}',k)\cdot\boldsymbol{J}(\boldsymbol{r}')\,dv' - \frac{\overline{\boldsymbol{L}}\cdot\boldsymbol{J}(\boldsymbol{r})}{j\omega\epsilon}. \tag{1}$$

In this expression, $\boldsymbol{r}, \boldsymbol{r}'$ are the observation and the source points, respectively, $k = \omega\sqrt{\epsilon\mu}$, $\boldsymbol{J}$ is the current density, $\overline{\boldsymbol{G}}_e$ is the dyadic Green's function of the electric type, V is the cavity volume, V_δ is a principal volume about $\boldsymbol{r}$ having dimensions proportional to δ, and, finally, $\overline{\boldsymbol{L}}$ is a constant dyadic which is determined only from the geometry of V_δ [1]. Numerical calculations of $\boldsymbol{E}$ may be performed conveniently using a generalization of (1), differing from it for V_δ being allowed to be finite and for the inclusion of a further integral over V_δ, involving $\overline{\boldsymbol{G}}_e$ [2].

Green's functions for bounded regions are usually given in the form of modal expansions, obtained by general procedures such as those described by Tai [3] and Felsen–Marcuvitz [4]. Examples of these expansions are given in [5]–[8] and in the next section. Though being of great theoretical interest, such modal series are unsuitable for use in numerical algorithms (moment method, for instance) which require the computation of the electric field inside the source region. In this case, indeed, the Green's function must be computed at points $\boldsymbol{r}'$ close to $\boldsymbol{r}$, where the convergence of the series is very poor due to the singularity of $\overline{\boldsymbol{G}}_e$ at $\boldsymbol{r}' = \boldsymbol{r}$. We recall that, in three-dimensional Green's functions, this singularity is of the order R^{-3}, where R is the distance between the source and the observation points.

This drawback can be avoided by using expressions where a diverging term, expressed in closed form, is extracted from the modal expansion of $\overline{\boldsymbol{G}}_e$, so that the remaining series represents a function finite at $\boldsymbol{r}' = \boldsymbol{r}$. This series, in fact, is expected to converge very well everywhere. In this paper, we deduce an expression of this type for a spherical resonator.

Manuscript received March 7, 1984; revised January 4, 1985.

The authors are with the Dipartimento di Elettronica dell'Università di Pavia, Strada Nuova 106/c, 27100 Pavia, Italy.

0018-9480/85/0500-0407$01.00 ©1985 IEEE